PHYSICAL REVIEW B **70**, 125417 (2004)

Fluctuating field model for conduction electron spin resonance in graphite

D. L. Huber
Physics Department, University of Wisconsin-Madison, Madison, Wisconsin 53706, USA

R. R. Urbano, M. S. Sercheli, and C. Rettori
Instituto de Fisica "Gleb Wataghin," UNICAMP, Campinas, São Paulo, Brazil

(Received 11 May 2004; published 20 September 2004)

We outline a theory for conduction electron-spin resonance (CESR) in highly oriented pyrolytic graphite. The fundamental approximation is to treat the spin-orbit interaction as an effective field. In this approach, the shift in the g factor, which is associated with the mean value of the field, is related to the orbital susceptibility of the electrons. The linewidth comes from fluctuations in the effective field caused by the scattering of the electrons. The theory is used to interpret our CESR measurements.

DOI: 10.1103/PhysRevB.70.125417 PACS number(s): 76.30.Pk, 71.18.+y, 75.30.Cr

I. INTRODUCTION

Recently, there has been renewed interest in measurements of the electronic and magnetic properties of graphite. Some of these studies have revealed behavior that may not fit within the framework of an independent-electron model.[1–3] Among the probes that have been employed is conduction electron-spin resonance (CESR).[3–6] In these references, measurements of the temperature-dependent g factor and the linewidth were reported that showed significant asymmetry and temperature dependence below 200 K. The interpretation of the CESR results is uncertain.[7–9] According to Ref. 7, "a reliable theory for the g factor in graphite remains to be developed." The approach outlined in Ref. 9, which is the most detailed independent-electron theory to date, gives the wrong sign for the g shift when evaluated with positive spin-orbit parameters. Furthermore, the calculations of Ref. 9 deal only with the g factor and are unsuited to characterizing the resonance in regimes where electron-electron interactions are important. The purpose of this note is to outline a theory for the CESR g factor and linewidth in graphite that does not invoke the independent-electron approximation. The fundamental approximation is to treat the spin-orbit interaction as an effective field. In our approach, the shift in the g factor is related to the average value of the effective field while the linewidth is associated with the fluctuations in the effective field arising from the scattering of the electrons. We use the effective-field model to interpret our experimental results for the CESR g factors and linewidths in highly oriented pyrolytic graphite (HOPG).

II. CESR IN HOPG

In our approach to CESR in HOPG, we express the spin-orbit interaction in the single-orbital ($2p_z$), tight-binding limit where it is written $\Lambda\vec{l}\cdot\vec{s}$. The spin-dependent components of the static Hamiltonian take the form

$$H_S = 2\mu_B\sum_j s_{zj}H + \Lambda\sum_j \vec{l}_j\cdot\vec{s}_j. \tag{1}$$

Here s denotes the electron spin and l is the orbital angular momentum. Since the spin-orbit coupling in carbon is very weak, we treat the interaction as an effective field whose static and dynamic properties are those of an electron gas without spin-orbit interactions. If we add to H_S the orbital Zeeman term $\mu_B L_z H$, where L_z is the z component of the total orbital angular momentum, we obtain a Hamiltonian that is formally identical to the Hamiltonian of a system of exchange-couple unlike spins,[10–12] with the unlike spins being identified with the orbital moments. Because of this correspondence, we can make use of techniques developed in Refs. 10–12 in our analysis.

An essential assumption in our approach is that the fluctuations in the orbital moments, which can arise from both elastic- and inelastic-scattering processes, decay on a time scale τ, which is short in comparison with the precession period of the spins. This assumption, which is equivalent to the "rapid modulation limit," is what distinguishes our approach from previous calculations of the g factor which neglect the scattering processes and hence are equivalent to the "static" limit. As we will see below, the absence of significant frequency dependence in the linewidth supports such an assumption.

We begin by introducing the Fourier expansions of the local spin and orbital operators:

$$\vec{s}_j = N^{-1}\sum_{\vec{k}} e^{i\vec{k}\cdot\vec{r}_j}\vec{S}(\vec{k}), \tag{2}$$

$$\vec{l}_j = N^{-1}\sum_{\vec{k}} e^{i\vec{k}\cdot\vec{r}_j}\vec{L}(\vec{k}), \tag{3}$$

where N denotes the number of electrons and the sum is over the Brillouin zone. The spin Hamiltonian takes the form

$$H_S = 2\mu_B S_z(0)H + \Lambda N^{-1}\sum_{\vec{k}} \vec{L}(-\vec{k})\cdot\vec{S}(\vec{k}). \tag{4}$$

We obtain the shift in the g factor from the equation of motion of the transverse component of the total spin $S_+(0)$ after replacing $L(-k)$ by its thermal average. In the presence of a uniform magnetic field directed along the z axis, only $\langle L_z(0)\rangle$ survives the thermal averaging. Writing $g(T)=2+\Delta g(T)$, we have for the g shift,

$$\Delta g = \Lambda\langle L_z(0)\rangle/N\mu_B H = -\Lambda\langle m_z\rangle/\mu_B^2 H. \quad (5)$$

Here $\langle m_z\rangle$ is the average orbital magnetic moment per resonating electron, and we have utilized the result that the magnetic moment is antiparallel to the angular momentum.[13] The ratio $\langle m_z\rangle/H$ defines the fixed-field, single-electron orbital susceptibility which we identify with the ratio of the bulk fixed-field orbital susceptibility, $\chi_{\rm orb}(T,H) \equiv M(T,H)/H$, to an effective electron density $N_{eff}(T,H)$. We thus obtain

$$\Delta g(T) = \frac{-\Lambda\chi_{orb}(T,H)}{\mu_B^2 N_{eff}(T,H)}. \quad (6)$$

Equation (6) is our final result for the shift in the g factor. Although we defer comparison with experiment until later, we note that the orbital susceptibility in HOPG is largest when the field is parallel to the c axis. As a consequence, the g shift in the parallel configuration is much greater than when the field is perpendicular to the c axis. Because $\chi_{\rm orb\|}$ is negative, the corresponding g shift is positive since the spin-orbit parameter Λ is positive.

In the analysis of the linewidth, we make use of a general expression for T_2 derived previously.[14] In Ref. 14, the anisotropic terms in the spin Hamiltonian gave rise to the linewidth. In the present problem that role is played by the spin-orbit interaction since it does not commute with the total spin. We have

$$1/T_2 = \frac{\mu_B^2}{kTV\hbar^2\chi_S(0)} \times \int_{-\infty}^{+\infty} dt\langle\{[S_+(0,t),H_{so}(t)],[H_{so}(0),S_-(0,0)]\}\rangle. \quad (7)$$

Here $\chi_S(0)$ denotes the uniform-field spin susceptibility, V is the volume, H_{so} is the spin-orbit interaction appearing in Eq. (4) and the curly brackets denote a symmetrized product.

The commutators in Eq. (7) have the form

$$\left[S_\pm(0), \Lambda N^{-1}\sum_{\vec{k}} \vec{L}(-\vec{k})\cdot\vec{S}(\vec{k})\right] = \mp\Lambda N^{-1}\sum_{\vec{k}} L_z(-\vec{k})S_\pm(\vec{k}) \pm \Lambda N^{-1}\sum_{\vec{k}} L_\pm(-\vec{k})S_z(\vec{k}). \quad (8)$$

As will be discussed below, we expect that when the static field is along the c axis the dominant contribution to the linewidth comes from the first term on the right hand side of Eq. (8), i.e., the longitudinal fluctuations in the orbital angular momentum. Consistent with the weak coupling approximation, we factor the spin and orbital terms in the correlation function in Eq. (7), obtaining an expression of the form

$$\sum_{\vec{k}} \langle S_+(\vec{k},t)S_-(-\vec{k},0)\rangle\langle L_z(-\vec{k},t)L_z(\vec{k},0)\rangle.$$

If we further assume that the decay time for the momentum correlations (see above) satisfies the condition $\omega\tau \ll 1$, where $\omega/2\pi$ is the precession frequency of the spins, then the integrand becomes $(k_BTV/2\mu_B^2)\Sigma_{\vec{k}}\chi_S(\vec{k})\langle\{L_z(-k,t),L_z(k,0)\}\rangle$. where $\chi_S(k)$ denotes the wave-vector dependent static spin susceptibility. After making these approximations, the linewidth takes the form

$$1/T_2 = \frac{\Lambda^2}{2\hbar^2\chi_S(0)} N^{-1}\sum_{\vec{k}} \chi_S(\vec{k})\int_{-\infty}^{\infty} dt\langle\{L_z(-\vec{k},t),L_z(\vec{k},0)\}\rangle. \quad (9)$$

Equation (9) is our final result in which the linewidth is expressed as a sum over k, weighted by the k-dependent static spin susceptibility of a time integral over a k-dependent orbital angular moment correlation function. We postpone discussion of this equation until after we present our experimental findings.

III. EXPERIMENTAL RESULTS

Experimental results for the resonance field, the linewidth, and $g_\|$ for HOPG were reported in Ref. 3 for Q, X, and S-band frequencies. In this section we present additional X-band data for the g factors and linewidths as well as fixed-field susceptibility measurements on the same sample used in the CESR work which was synthesized at the Research Institute "Graphite" (Moscow). The data were taken with a Bruker ELEXSYS-CW spectrometer at X-band frequency using a TE_{102} room temperature cavity and a He gas flux temperature controller. Figure 1 displays the X-band (9.482 GHz) data between 4.2 K and 300 K. In both configurations, $H\|c$ and $H\perp c$, the microwave and dc-magnetic fields were kept mutually perpendicular in order to achieve maximum microwave penetration to avoid a line shape change caused by anisotropic skin depth effects.[15] In all cases, the line shape was Dysonian indicating conducting behavior of the sample.

Figure 1 displays the linewidth and g factor data for both the parallel and perpendicular configurations. It is evident that $g_\perp$ is essentially constant and close to the free-electron value of 2.0023. In contrast, $g_\|$ is $\approx$2.05 at 300 K and increases to a value close to 2.16, before leveling off. The linewidth data for $H\|c$ increase rapidly with decreasing temperature, reaching a value $\sim$95 Oe at 10 K; in contrast, the linewidth for $H\perp c$ increases much less rapidly, reaching a maximum of 30 Oe before showing a slight downturn.

Figure 2 shows the results for the fixed-field bulk susceptibility (M/H) at a field of 3400 Oe for both the parallel and perpendicular configurations. Note that this value of the field corresponds to a resonance at 9.482 GHz with a g factor equal to 2. The measurements were carried out in a Quantum Design SQUID MPMS-5 magnetometer in the temperature range between 2 K and 300 K. The susceptibility for $H\|c$ decreases rapidly from room temperature approaching a minimum of -2.94×10^{-5} emu/g at 34 K before increasing to -2.82×10^{-5} emu/g at 2 K. The fixed-field susceptibility for $H\perp c$ is also negative but much smaller in magnitude than $\chi_\perp$. The ratio of $\chi_\|/\chi_\perp$ varies from 55 at 300 K to 104 at 5 K. Note that the measured susceptibilities, $\chi_\|$ and $\chi_\perp$, also have contributions from the diamagnetic core suscepti-

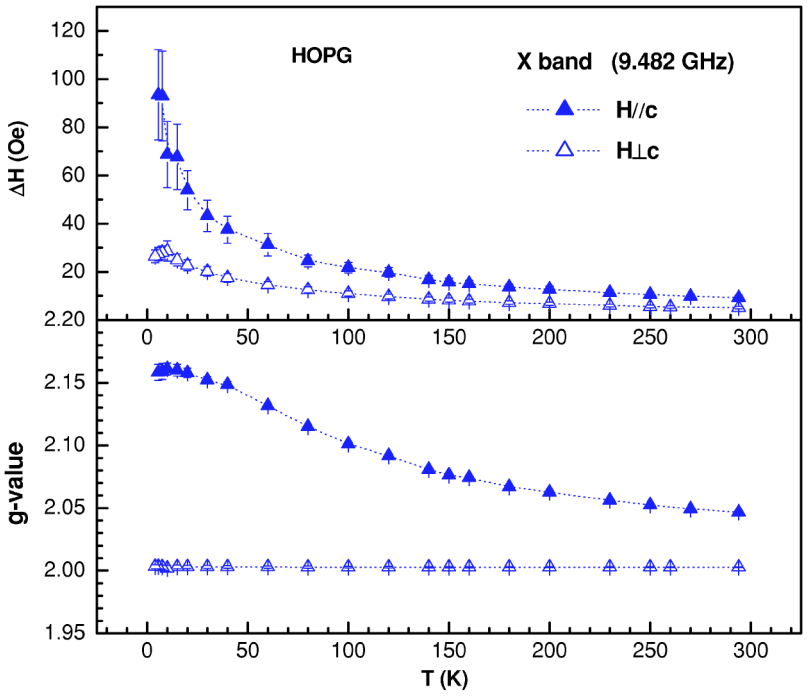

FIG. 1. (Color online) Linewidths and g values with applied fields parallel (solid triangles) and perpendicular (open triangles) to the c axis of HOPG. The measurements were carried out at X-band frequency, 9.482 GHz. The dotted curves are guides to the eye.

bility and the paramagnetic Pauli susceptibility of the carriers, both of which are isotropic.[16] According to Ref. 16, the former is on the order of -0.04×10^{-5} emu/g, which is comparable to our measured values of $\chi_\perp$, while the latter is estimated to be much smaller, 0.0016×10^{-5} emu/g.

IV. DISCUSSION

The theory outlined above establishes a connection between the g shifts and the orbital components of the fixed-field susceptibilities. The behavior of the bulk susceptibilities shown in Fig. 2 is *qualitatively* consistent with the variation of the g values shown in Fig. 1. Since $\chi_{orb}\|\chi_{orb}>100$ at low temperatures, one expects $\Delta g_\perp$ to be smaller than $\Delta g_\|$ by about the same factor, i.e., $\Delta g_\perp \leqslant 0.002$. Because $\Delta g_\perp$ is small, it is difficult to distinguish the contribution of the orbital susceptibility [Eq. (5)] from intra-atomic contributions and vacuum fluctuation effects.

The ratio of the parallel g shifts at the limiting temperatures, $\Delta g_\|(2\text{ K})/\Delta g_\|(300\text{ K})\approx 3$, is greater than one would expect from the ratio of the susceptibilities, $\chi_\|(2\text{ K})/\chi_\|(300\text{ K})\approx 1.5$. We attribute this to the temperature variation of the effective electron density N_{eff}. In graphite, neither the value of N_{eff} nor Λ is known.[17] It is important to

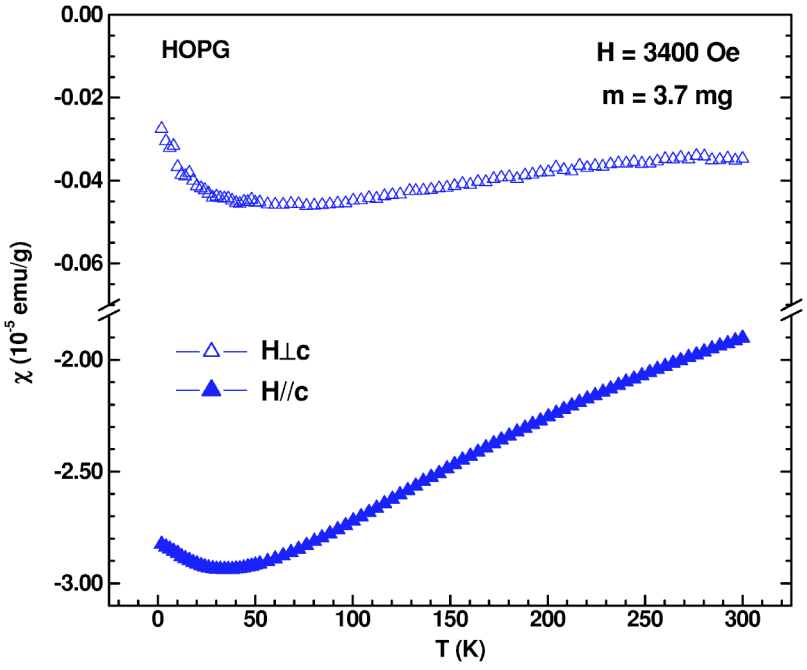

FIG. 2. (Color online) Fixed-field susceptibilities for applied fields parallel (solid triangles) and perpendicular (open triangles) to the c axis of HOPG. The fixed-field susceptibility is defined as the ratio of the bulk magnetization to the field in an applied field of 3400 Oe. Note the change in vertical scale between the upper and lower curves.

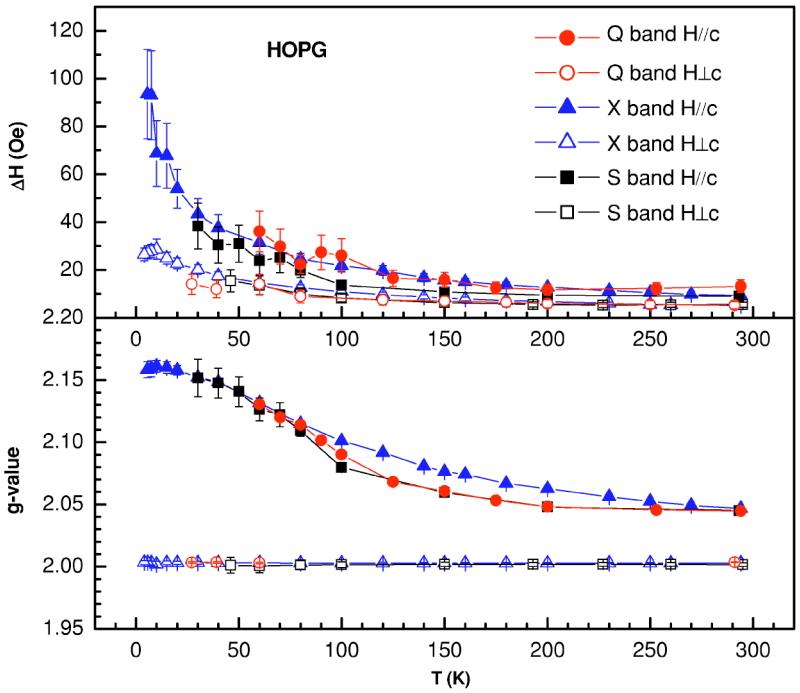

FIG. 3. (Color online) Linewidths and g values in the parallel and perpendicular configurations for S-band, X-band, and Q-band frequencies. Note the difference between the X-band and the S- and Q-band values of $g_{\|}$ between 100 K and 300 K.

keep in mind that our effective electron density is defined by the ratio $H\chi_{\|}/\langle mz\rangle$ and is not identical to the carrier density inferred from transport measurements, although it is reasonable to expect similar temperature variations in the two parameters. The decrease in $\Delta g_{\|}$ from 0.15 at 50 K to 0.05 at room temperature, together with the increase in $\chi_{orb\|}$ from -2.9×10^{-5} emu/g to -1.9×10^{-5} emu/g over the same temperature range, is consistent with an increase in N_{eff} by a factor of 2. The fractional increase is comparable to the increase in the carrier density over the same temperature range.[18]

From Eq. (9) it is evident that the behavior of $1/T_2$ is determined by the time integral of a correlation function associated with the *fluctuations* in the orbital angular momentum. At low temperatures, where $|\chi_{\|}|$ becomes large, it is expected that the amplitudes of the longitudinal fluctuations increase. It is also expected that the fluctuations will decay more slowly, corresponding to an increase in the correlation time. Both of these effects contribute to the increase in the linewidth as $T\rightarrow0$.

From Fig. 1, it is apparent that there is also a small increase in linewidth when the static field is perpendicular to the c axis. A possible explanation for this effect follows from Eq. (7). In addition to the longitudinal terms, the linewidth has contributions from the fluctuations in the orbital momentum that are perpendicular to the applied field. When the static field is parallel to the c axis, the perpendicular fluctuations are small ($\chi_{\perp}/\chi_{\|}\ll1$) and their contribution to the linewidth at low temperatures is probably negligible. When the static field is perpendicular to the c axis, however, there is a contribution to the linewidth coming from the *transverse fluctuations that are directed along the c axis*. Although the c-axis fluctuations are suppressed by the perpendicular field, if the suppression is not complete, they may be giving rise to the weak growth in $\Delta H_{\perp}$ as $T\rightarrow0$.

With $H\|c$, the dominant fluctuations in the effective field are along the direction of the dc field. Under these conditions, the linewidth is due almost entirely to dephasing effects. As a consequence, one has $T_1\gg T_2$, where T_1 and T_2 are the longitudinal and transverse relaxation times, respectively. When one has $H\perp c$, the c axis fluctuations are perpendicular to the applied field. If the c axis fluctuations were still dominant, one would have largely lifetime broadening, i.e., $T_2\approx2T_1$; more generally, one expects that $T_1<T_2<2T_1$.

We have also made measurements of the parallel and perpendicular g factors and linewidths at S band (4 GHz) and Q band (34.4 GHz) frequencies. These results, along with the X band data, are shown in Fig. 3. The X- and S-band (and Q-band for $T\geqslant125$ K) linewidths are nearly identical, as is to be expected in the rapid modulation limit, where $\omega\tau\ll1$. Additional evidence in support of the rapid modulation approximation comes from measurements of the resistivity reported by Du *et al.* in Ref. 2. From the transport data, they infer a carrier scattering time associated with electron-phonon interactions on the order of $1.7\times10^{-10}\ T^{-1}$ s (T in K). Although caution is called for in utilizing scattering times inferred from transport measurements to interpret CESR data, it appears that the rapid modulation limit is appropriate for S- and X-band measurements down to temperatures on the order of 10 K or below. In the case of Q-band studies, the breakdown of the rapid modulation limit may begin to occur at higher temperatures (50 K–100 K).

It should be noted that there is a small difference between the X-band and the S- and Q-band g factors in the parallel configuration over the range $100\ \text{K}\leqslant T\leqslant250$ K. This difference, which is also seen in other HOPG samples, occurs in a region where the bulk susceptibility is field independent for the resonance fields used in the experiment. Within the effective-field model, such a shift is associated with differences in the effective electron density N_{eff}. This effect does not appear to be an experimental artifact since our X-band data for $g_{\|}$ are very similar to the values of $g_{\|}$ reported in Ref. 9.

As mentioned previously, we used the tight binding or atomic approximation for the spin-orbit interaction. The general expression for the spin-orbit interaction takes the form $(\hbar/2m^2c^2)(\nabla V\times\vec{p})\cdot\vec{s}$, where V is the periodic potential and p is the electron momentum. The axial vector $\nabla V\times\vec{p}$ has the same transformation properties as the orbital angular momentum. With the more general form of the interaction, the g shift is given by

$$\Delta g = (\hbar/2m^2c^2)\langle(\nabla V\times\vec{p})_z\rangle/\mu_B H. \tag{10}$$

Here the brackets denote a thermal average over the manifold of hybridized $2p$ states contributing to the dynamic spin susceptibility. If the tight-binding approximation is appropriate, the variation of $\langle(\nabla V\times\vec{p})_z\rangle$ with field and temperature should be similar to that of $\langle l_z\rangle$.

In summary, in the fluctuating field model for CESR in HOPG, the anomalous g shift and linewidth that are observed with the static field along the c axis are associated with the longitudinal fluctuations in the orbital angular momentum [or its generalization $(\nabla V\times\vec{p})$]. The g shift is related to the static orbital susceptibility, which characterizes the equal-time correlations of the orbital moments, whereas the linewidth is related to the dynamical correlations. The theory predicts that the ratio $\Delta g_{\|}/\Delta g_{\perp}$ is equal to $\chi_{orb}/\chi_{orb\perp}$. Unfortunately, it has not been possible to test this prediction because $\Delta g_{\perp}$ is too small to separate the orbital part from various temperature-independent contributions. Although we do not have a detailed prediction for the magnitude and temperature dependence of the linewidth, it may be possible to check the predictions for the relative magnitudes of T_1 and T_2 in the parallel and perpendicular directions discussed above.

As a final point, we mention that the approach outlined here for graphite may also be useful for interpreting CESR in carbon nanotubes. Although there are predictions for unusual behavior in single-wall and multiwall nanotubes,[19] the experimental evidence seems to support the interpretation that the ESR in single-wall nanotubes is associated with paramagnetic defects.[20] In the case of multiwall nanotubes, a variety of behaviors is found.[20] We expect our theory to be applicable to those samples where the line shape is Dysonian indicating conducting behavior of the resonant electrons.

ACKNOWLEDGMENTS

We would like to thank Professor Yakov Kopelevich for interesting discussions and for providing the sample used in the measurements.

[1] Y. Kopelevich, J. H. S. Torres, R. R. da Silva, F. Merowka, H. Kempa, and P. Esquinazi, Phys. Rev. Lett. **90**, 156402 (2003); see also S. Moehlecke, Y. Kopelevich, and M. B. Maple, Phys. Rev. B **69**, 134519 (2004).

[2] For alternative indepdent-electron interpretations of the magnetotransport data in HOPG see T. Tokumoto, E. Jobilong, E. S. Choi, Y. Oshima, and J. S. Brooks, Solid State Commun. **129**, 559 (2004); X. Du, S.-W. Tsai, D. L. Maslov, and A. F. Hebard, cond-mat/0404725 (unpublished).

[3] M. S. Sercheli, Y. Kopelevich, R. R. da Silva, J. H. S. Torres, and C. Rettori, Solid State Commun. **121**, 579 (2002).

[4] G. Wagoner, Phys. Rev. **118**, 647 (1960).

[5] L. S. Singer and G. Wagoner, J. Chem. Phys. **37**, 1812 (1962).

[6] K. Kawamura, S. Kaneko, and T. Tsuzuku, J. Phys. Soc. Jpn. **52**, 3936 (1983).

[7] M. S. Dresselhaus, G. Dresselhaus, K. Sugihara, I. L. Spain, and H. A. Goldberg, *Graphite Fibers and Filaments*, *Springer Series in Materials Science* (Springer-Verlag, Berlin, 1988), Vol. 5, p. 183.

[8] A. S. Kotosonov, Zh. Eksp. Teor. Fiz. **93**, 1870 (1987) [Sov. Phys. JETP **66**, 1068 (1987)].

[9] K. Matsubara, T. Tsuzuku, and K. Sugihara, Phys. Rev. B **44**, 11845 (1991).

[10] H. Hasegawa, Prog. Theor. Phys. **21**, 483 (1959).

[11] H. Cottet, P. Donzé, J. Dupraz, B. Giovannini, and M. Peter, Z. Angew. Phys. **24**, 249 (1968).

[12] D. L. Huber, Phys. Rev. B **13**, 291 (1976).

[13] J. H. Van Vleck, *Electric and Magnetic Susceptibilities* (Oxford University Press, London, 1932), Chaps. 1,6.

[14] D. L. Huber, G. Alejandro, A. Caneiro, M. T. Causa, F. Prado, M. Tovar, and S. B. Oseroff, Phys. Rev. B **60**, 12155 (1999).

[15] L. Walmsley, G. Ceotto, J. H. Castilho, and C. Rettori, Synth. Met. **30**, 97 (1987).

[16] M. S. Dresselhaus and G. Dresselhaus, Am. J. Optom. Physiol. Opt. **30**, 139 (1981).

[17] As a point of reference, the spin-orbit parameter in atomic boron, which has a single $2p$ electron, is 1.3 meV [C. E. Moore, Natl. Bur. Stand. Circ. (U. S.) **467**, 16 (1949)]. With this value for Λ, one obtains 10^{22} cm^{-3} for the effective electron density at 2 K.

[18] R. O. Dillon, I. L. Spain, J. A. Woolam, and W. H. Lowrey, J. Phys. Chem. Solids **39**, 907 (1978).

[19] A. De Martino, R. Egger, K. Hallberg, and C. A. Balseiro, Phys. Rev. Lett. **88**, 206402 (2002).

[20] K. Shen, D. L. Tierney, and T. Pietrass, Phys. Rev. B **68**, 165418 (2003).